Research Article

Self-Assembled rGO/$FeWO_4$ Flower Structures by a Solvothermal Reaction with Enhanced Catalytic Activity for Dye Degradation

G. Jenita Rani, S. M. Sathiya and M.A. Jothi Rajan*

Bio- Nano Laboratory, Research Department of Physics, Arul Anandar College, Karumathur, Madurai- 625 014, India

Abstract

This work reports the synthesis of reduced graphene oxide/iron tungstate (rGO/$FeWO_4$) nanocomposite and explores the catalytic activity toward Methyl Orange (MO) dye degradation. The composite formation of rGO sheets with $FeWO_4$ nanostructures was achieved by a simple process of one-step solvothermal strategy. The flower like morphology of $FeWO_4$ densely covered by the rGO sheets was revealed from the SEM. The crystalline nature and monoclinic primitive structure of prepared $FeWO_4$ nanomaterials was confirmed from the diffraction patterns and the nucleation sites exploited for the composite formation of $FeWO_4$ nanostructures with rGO sheets was explored by using FT-IR spectroscopy. The catalytic activity of prepared nanostructures toward MO dye degradation in the presence of $NaBH_4$ was evaluated, in which rGO/$FeWO_4$ composite exhibited the remarkable catalytic activity toward MO degradation. The synergetic effects of composite such as high surface area, exposed catalytically active sites and enhanced transfer of hydrogen species contribute to the superior catalytic activity of rGO/$FeWO_4$ and the involved degradation reaction followed a pseudo first order kinetics.

Keywords: solvothermal, hierarchical structure, electron relay, catalytic activity, methyl orange.

***Correspondence**

Author: M. A. Jothi Rajan

Email: anjellojothi@gmail.com

Introduction

The incessant growth in the industrialization and urbanization of modern human society has its adverse impact on the environment. The industrial contaminants such as oil spillage, nitroaromatic compounds, chlorinated solvents, organic wastes, phenols and synthetic dyes affect the water sources and endanger the mere survival of aquatic living organism in a cleaner ambience [1-3]. Among the various type of dye contaminants present in the water sources, Methyl orange (MO) is one of the stable, toxic, and recalcitrant azo dye which can cause carcinogenic and mutagenic effect to living organisms [4]. Thus, the effective treatment of these dye effluents before being disposed into environment is of major concern and crucial need of the hour. Hence, number of techniques such as chlorination, ozonation, adsorption and biodegradation has been extensively explored for the degradation of MO dye [5-7]. However, the above methods involved certain limitations including cost effectiveness, inadequacy in dye removal, phase change of pollutant, resistivity of dye towards microorganisms and difficulty in disposal. Hence, there is an intense necessity to develop a cheaper, biocompatible and highly efficient catalyst material that aid the faster degradation of MO dye. Recently, metal and metal oxide nanoparticles have emerged as hot topic of interest in dye degradation field owing to their unique electrical, optical and catalytic properties. Metal nanoparticles such as Au [8], Ag [9], Fe [10], Cu [11], Ni [12] and metal oxide nanopaticles TiO_2 [13], ZnO [14], ZnS [15], CdS [16] are some of the most commonly studied catalyst materials to degrade the dye molecules. Although these catalysts exhibited fine activity, the loss of suspended nanoparticles and their complicated recycling steps hampered the effective usage of these materials for large scale application. In addition, the usage of toxic organic solvents and complex reaction conditions involved in the synthesis process of some these materials add to the inconvenience of practical usage.

Tungstate (WO_4), being one of the significant inorganic material has found its wide application in optical fibers, laser hosts, catalysts, photoluminescence and microwave applications [17, 18] because of its specific structural and optical properties. Particularly, iron tungstate ($FeWO_4$), also known as ferberite, consisting of hexagonally close-packed oxygen with metal cations occupying some of the octahedral sites in an orderly manner, has been exploited as

photocatalytic entrant due to its narrow band gap and good electron transport property. Zhou et al reported the photocatalytic activity of $FeWO_4$ for the degradation of Rhodamine B under UV and visible light irradiation [19]. Chen et al investigated on $H_2O/H_2O_2/FeWO_4$ system for H_2 evolution under solar light and visible light [20]. Guo et al made a comparative photodegradation study on $FeWO_4$ and TiO_2 [21]. Although a notable degradation activity was observed in the above reports, the reaction required a large quantity of catalyst material and a longer time of exposure to UV/visible light to activate the catalyst. A simple, alternate and eco-friendly approach has been adopted in this work for the elimination of toxic dye and to convert them into harmless end product through catalytic reduction in the presence of $NaBH_4$. However the solitary use of $FeWO_4$ as catalyst material often resulted in loss of active sites and agglomeration of catalyst in aqueous solution, which led to the substantial reduction of catalytic activity. To overcome this drawback, $FeWO_4$ nanoparticles could be effectively hybridized with a carbon support to make a composite, which blends the advantages associated with the intrinsic property of carbon materials with $FeWO_4$ to provide a superior catalytic activity. Graphene, as an active carbon support, has captured immense attention, owing to its high surface area, charge carrier mobility, excellent electron transport property, good chemical stability and superior catalytic activity [22, 23]. This flat monolayer of carbon atoms tightly bound into a 2D honeycomb lattice, not only act as a volume buffer but also preserve the catalytically active sites, while preventing the aggregation of nanoparticles [24]. The adsorption capacity of rGO/ $FeWO_4$ is enhanced through spacing effect between $FeWO_4$ and graphene sheets which may lead to the high catalytic performance of the composite toward MO dye.

The objective of this work is to synthesis rGO/$FeWO_4$ nanostructures through a simple, one-step, solvo-thermal method and to evaluate its catalytic efficiency toward MO dye degradation.

Experimental

Materials

Iron (III) chloride hexahydrate ($FeCl_3.6H_2O$, AG, ≥ 97.0, Alfa Aesar), sodium tungstate dihydrate ($Na_2WO_4.2H_2O$, AG, ≥ 99%, Sigma Aldrich), ethylene glycol ($C_2H_6O_2$, AR, ≥ 99%, Merck), sodium acetate ($C_2H_3NaO_2$, AG ≥ 99%, Merck), graphite powder (≥ 99.99%, Sigma Aldrich), methyl orange ($C_{14}H_{14}N_3NaO_3S$, ACS reagent, 85%, Sigma Aldrich), sodium borohydride ($NaBH_4$, powder, ≥ 98%, Sigma Aldrich) were used without further purification.

Preparation of $FeWO_4$ nanoparticles

2 M $FeCl_3.6H_2O$ and 2 M of $Na_2WO_4.2H_2O$ were dissolved in a mixture solution of $C_2H_6O_2$ and H_2O_2 ($V_{H_2O_2}/V_{EG}$ = 2:8) which was followed by the addition of 1 M $C_2H_3NaO_2$ and the said solution was magnetically stirred for 1 h. The solution was transferred into a Teflon-lined stainless steel autoclave and heated in an electric oven at 200 ºC for 10 h, and cooled to room temperature. The resultant product was separated *via* centrifugation, washed with de-ionized water and absolute ethanol for several times and dried at 60 °C for 6 h.

Preparation of rGO/ $FeWO_4$ composite

Graphite powder was converted into GO by using the modified Hummer's method [25]. To the GO dispersion, a mixture solution of $C_2H_6O_2$ and H_2O_2 ($V_{H_2O_2}/V_{EG}$ = 2:8) containing 2 M $FeCl_3.6H_2O$ and 2 M $Na_2WO_4.2H_2O$ was gradually added. 1 M $C_2H_3NaO_2$ was introduced into the above solution and magnetically stirred for 1 h. Then the solution was transferred to a 50 ml Teflon-lined stainless steel autoclave and heated at 200 ºC for 10 h. Subsequently, the product was centrifuged and washed with de-ionized water and absolute ethanol for several times and dried at 60 °C for 6 h.

Material characterizations

The prepared nanostructures were characterized using a TESCAN VEGA3 SBU - scanning electron microscopy (SEM), RIGAKU MINIFLEX II C - X-ray powder diffractometer (XRD) and SHIMADZU-EQUINOX – FT-IR spectroscopy.

MO dye degradation experiment

The catalytic activities of prepared nanostructures toward MO were evaluated experimentally by adding 3×10^{-2} M $NaBH_4$ solution in the 5×10^{-5} M MO dye solution. 5 mg of the prepared catalyst was added to the above mixture and magnetically stirred for different time intervals. The catalyst from the solution was separated by centrifugation and the concentration of remnant MO in dye solution was spectrophotometrically monitored by measuring the absorbance at 465 nm through UV-*Vis* spectrophotometer.

Results and Discussion

Morphological properties

The morphological features of prepared nanostructures were studied by using SEM and the images are shown in **Figure 1**. The SEM images of $FeWO_4$ (Figure 1a and b) displayed a numerous flower like particles, each flower consisting of six symmetric petals in three dimensional view with the size range of 2-5 µm. From the high magnified view of the single flower, it is evident that each flower is composed of a pile of layers assembled hierarchically to make flower structure. The hierarchical flower structure formation of $FeWO_4$ consists of two stages: Primarily, a binary solvent system consisting of H_2O in Ethylene Glycol (EG) is employed for dissolving the iron and tungstate precursors. The H_2O molecule in this "quasi-reverse-emulsion" system interacted among themselves through hydrogen bonding and formed a water-rich region [26].

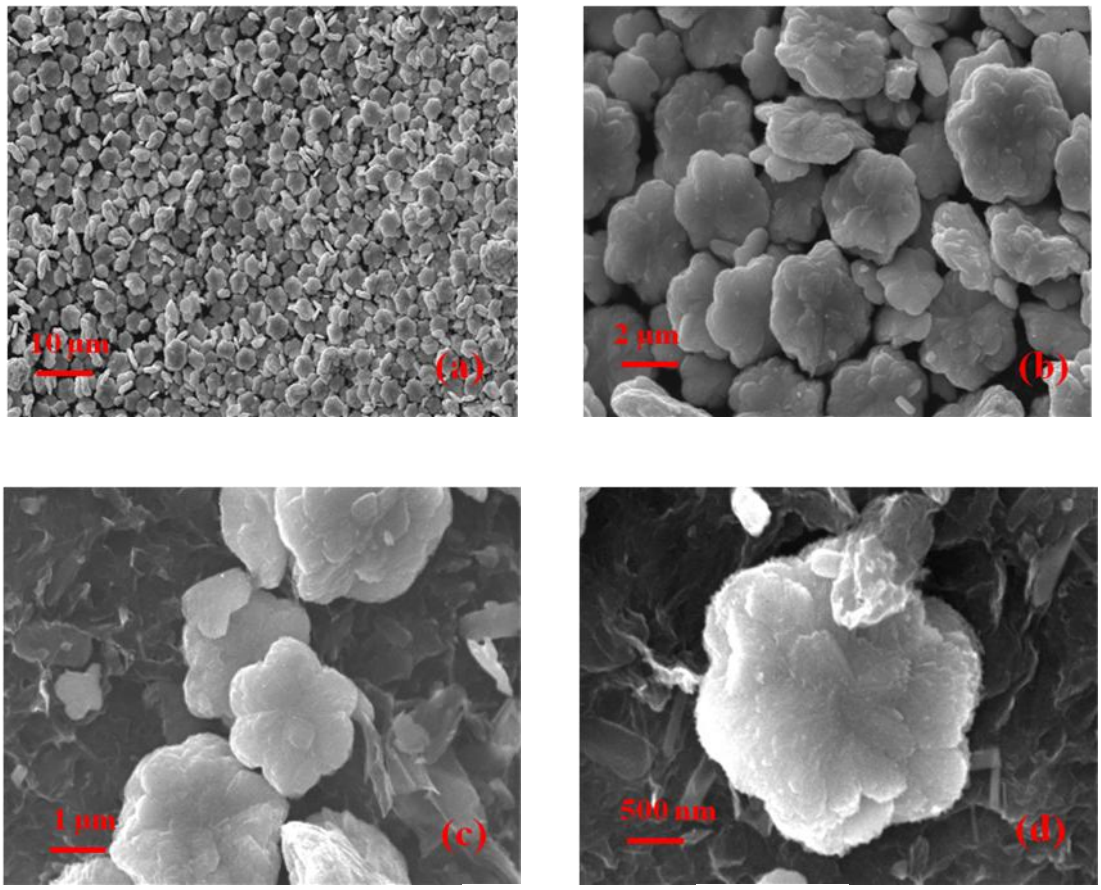

Figure 1 SEM images of (a), (b) $FeWO_4$ and (c), (d) rGO/$FeWO_4$ nanosturctures.

These water-rich regions created a local change in the chemical environment, which aided the transformation of the precursor materials into primary $FeWO_4$ nanocrystals. EG in the binary solvent is believed to play a triple role in the formation of flower like of $FeWO_4$. Since EG possesses the alike nature of H_2O, it has the capacity create hydrogen bonded-network, through which it become compatible with H_2O as co-solvent in the synthesis process [27]. Further, EG play a role of reducing agent and assist the reduction of Fe^{3+} ions into Fe^{2+} in the formation of $FeWO_4$.

Also, it acts as the crystal growth modifier and gives rise to the hierarchical structure $FeWO_4$. Sodium Acetate in the reaction mixture effects its role as precipitating agent and creates an alkaline atmosphere for the precipitation of newly formed $FeWO_4$ primary nanocrystals [19]. Secondarily, due to the temperature involved in solvothermal reaction, the primary nanocrystals of size 30-50nm aggregated to form thin layers of nanopetals. As the reaction proceeded for 10 h in a relatively high temperature, these thin layer assembled themselves into a pile of layer and gave rise to a well-defined, 3 dimensional flower nanostructure. The SEM images of rGO- $FeWO_4$ (Figure 1c and d) clearly exhibited that each $FeWO_4$ microspheric flower wrapped with a thin layer of graphene sheet. The chemically reduced GO contains multiple functional groups on the surface, which make it negatively charged [28], so that the $FeWO_4$ structures with positive surface charge can interact with rGO through electrostatic binding and physisorption to create unique rGO/ $FeWO_4$ structures.

The EDAX patterns of $FeWO_4$ and rGO/$FeWO_4$ are shown in **Figure 2a** and b. The $FeWO_4$ pattern indicates the obtained product is composed of Fe, W and O elements with atomic ratio 13.31:12.17:74.53 which is consistent with the stoichiometric ratio. In addition to the Fe, W and O elements with atomic ratio 6.41: 5.18: 60.85, rGO/$FeWO_4$ pattern manifested the presence of 27.56% of carbon which ensured the composite formation.

XRD patterns

The typical XRD patterns for $FeWO_4$ and rGO/$FeWO_4$ are shown in **Figure 3**. The well crystalline phase of obtained products is revealed through the strong and sharp peaks of XRD patterns. All the diffraction peaks for $FeWO_4$ (Figure 3a) can be ascribed to the monoclinic primitive structure with a space group p2/c and unit cell parameters of a = 4.750 A^0, b = 5.720 A^0, c = 4.970 A^0 and β = 90.17 (JCPDS card no. 71-2391) [29]. The diffraction pattern of GO (Figure 3b) manifested (001) reflection plane at 10.27^0, confirming the formation of GO nanostructure from graphite power [30]. The major peaks of $FeWO_4$ appeared to be same and reflection plane of GO was disappeared in for rGO/$FeWO_4$ composite (Figure 3c), specifying the reduction of GO. The presence of GO in the composite has not varied the crystalline phase and the crystallinity of $FeWO_4$.

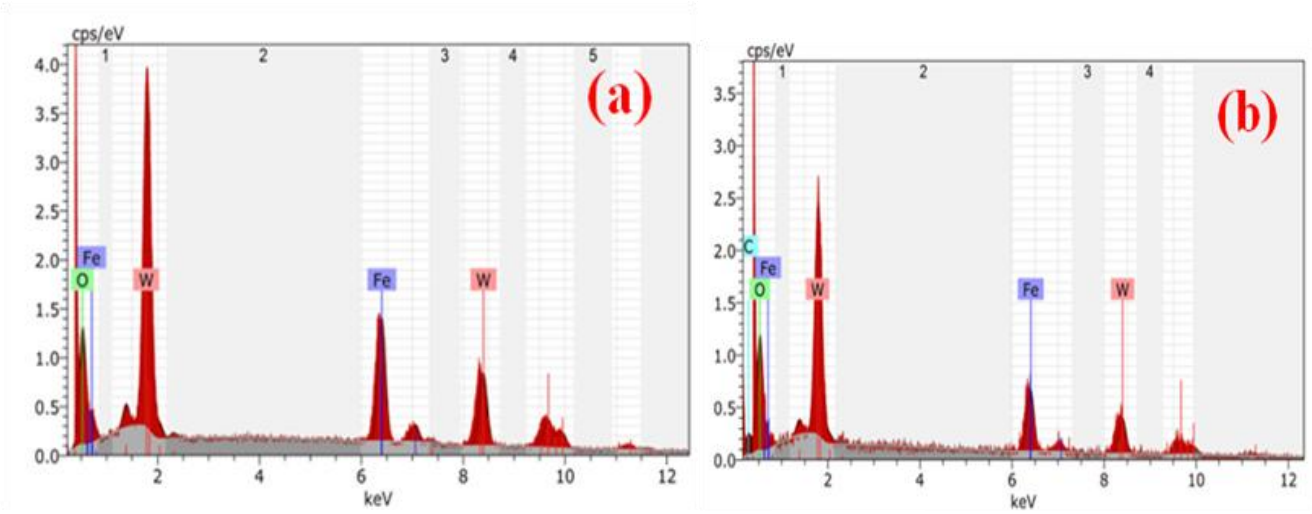

Figure 2 EDAX patterns of (a) $FeWO_4$ and (b) rGO/$FeWO_4$ nanosturctures.

FTIR

Figure 4a reports the FT-IR spectrum of $FeWO_4$ in which the absorption band at 652 cm^{-1} correspond to W-O stretching mode in WO_6 octahedral and the band at 832 cm^{-1} correspond to the symmetric vibration of oxygen atoms of Fe-O-W. The band at 510 cm^{-1} is ascribed to the asymmetric deformation of Fe-O in FeO_6 [31]. The FTIR spectrum of GO (Figure 4b) revealed C=O stretching vibration, ascribing to the carboxylic group present on the edges of GO at 1728 cm^{-1} and the C=C stretching vibration is found at 1634 cm^{-1}. The carboxyl and alkoxy groups are indicated through the C-O stretching vibrations atn1396 and 1096 cm^{-1} [32]. The rGO/ $FeWO_4$ conserved all the characteristic stretching vibrations corresponding to $FeWO_4$. The intensity of C=C, C-O and O-H stretching vibrations of GO found at 1634, 1096 and 3433cm^{-1}, respectively, is significantly reduced and the C-O stretching vibration at the 1396 cm^{-1}

was vanished in the prepared rGO/$FeWO_4$ composite (Figure 4c), representing that $FeWO_4$ nanosturctures were effectively anchored over the remaining carboxyl, epoxy, alkoxy and hydrophilic groups of rGO sheet [33].

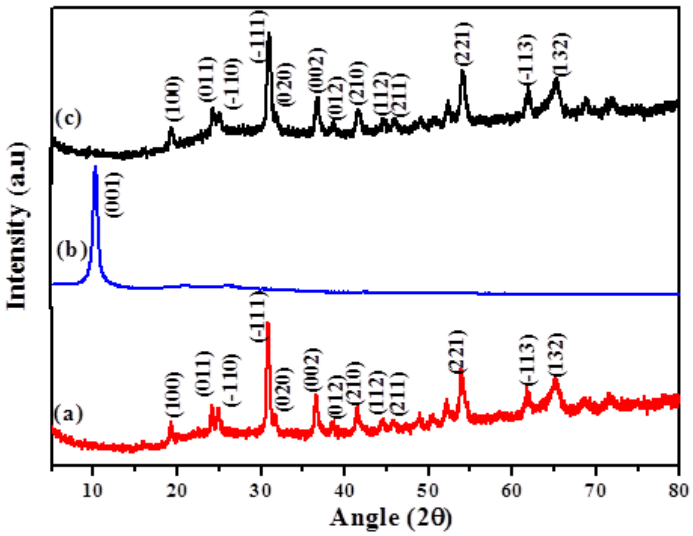

Figure 3 X-ray diffraction patterns of (a) FeWO4 (b) GO and (c) rGO/FeWO4 nanosturctures.

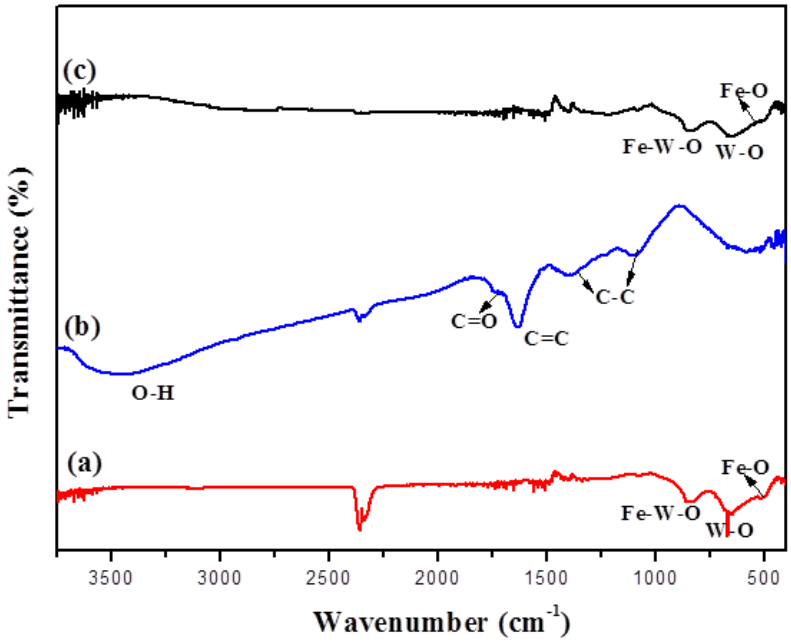

Figure 4 FT-IR spectra of (a) $FeWO_4$ (b) GO and (c) rGO/$FeWO_4$ nanosturctures.

MO degradation studies

The catalytic activities of prepared $FeWO_4$ and rGO/$FeWO_4$ nanostructures toward MO degradation in the presence of $NaBH_4$ were examined through UV-Vis spectroscopy and the corresponding SPR bands are ploted as a function of time (**Figure 5**). Beer-Lambert law A= ƐCl (where A is the absorbance of methyl orange dye, Ɛ is molar absorption coefficient, C is the concentration of dye and l is the path length of cell) was used to calculate the absorption of the dye solution.

The percentage of dye decomposition was calculated by using the formula:

$$\% \text{ of degradation} = \left(\frac{Co - Ct}{Co}\right) \times 100$$

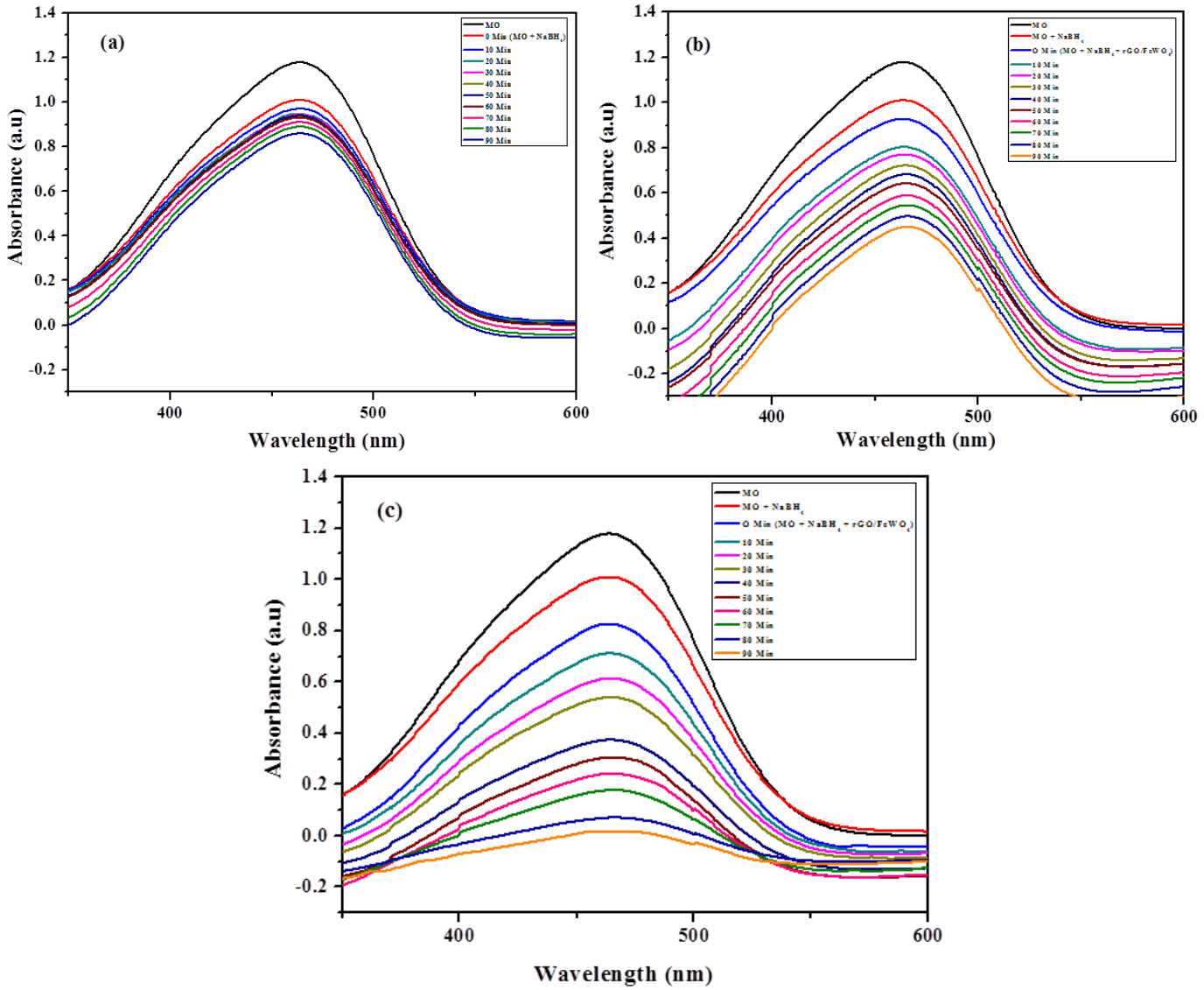

Figure 5 UV–Vis spectra of MB degradation process influenced by (a) $NaBH_4$ and $NaBH_4$ mediated (b) $FeWO_4$ (c) rGO/$FeWO_4$ nanosturctures observed at a equal time interval.

where C_o is the initial MB concentration and C_t is the concentration of MB at time t (**Figure 6**). MO exhibited its prominent SPR band at 465 nm due to the presence of azo group. Figure 5a showed the catalytic activity of $NaBH_4$ for the reduction of MO in the absence of any catalyst material. BH_4 anions present in $NaBH_4$ are nucleophilic in nature with high ability to supply electrons to the dye solution [34]. Hence, the absorption intensity of MO decreased by accepting electrons from BH_4 ions, but the reduction rate was very slow with minimum degradation 27.06% (Fig 5a and 6a) under given time constraint. It necessitates the requirement of catalytically active $FeWO_4$ material for an improved degradation of MO dye. $FeWO_4$ flower like structure exhibited unique characteristics of large surface area and highly reactive surfaces. The absorption efficiency is increased through the surface-to-volume ratio of $FeWO_4$, which is influential in the interaction of $FeWO_4$with MO dye molecule and BH_4 ions. $NaBH_4$ is believed to act as the source of hydrides [35] and assist $FeWO_4$ catalysts to activate the azo nitrogen bond of MO. They could also create a conjugation with the oxygen and sulphur atoms present in the dyes and weaken the azo double bond. Furthermore, the surface of $FeWO_4$ exhibit affinity toward hydrophilic organic MO dye and bring the dye molecules nearer to the catalytic sites, which led to the enhancement of dye degradation [35]. However, the degradation rate was limited to 61.81% in 90 min (Figure 5b and 6b) as $FeWO_4$ rapidly lost its active reaction site with MO dye due to the agglomeration of particles in an aqueous media, resulting inadequate chemical interaction of $FeWO_4$ with the dye molecule. The aforesaid limitation was easily tackled by the active rGO support on which nucleation and growth of

$FeWO_4$ was taken. The rGO sheet endowed with large high surface is capable of accommodating $FeWO_4$ nanosturctures with uniform distribution and hinders the physical aggregation of $FeWO_4$ under aqueous medium. Hence the active reaction sites of $FeWO_4$ are preserved to interact with dye molecules and simultaneously GO can adsorb MO dye on its surface. The decoration of $FeWO_4$ on rGO ensured good stability, high surface area, high catalytic performance and homogeneous environment which are essential for the enhanced catalytic activity. When the catalyst composite rGO/$FeWO_4$ was added to the reaction mixture, both BH_4 ions and MO dye molecules were adsorbed on the surface of the catalyst and the transfer of hydrogen species from the surface of BH_4 to the surface of MO through rGO/ $FeWO_4$ composite lead to the fast reduction of dye molecules. Since, the rGO is an effective electron acceptor and transporter, rGO/$FeWO_4$ could function as electron relay system between BH_4 donor and MO acceptor [36] and facilitate the fast electron transfer and decompose the dye molecules in comparison with the bare $FeWO_4$ catalyst. Apparently, the rGO/ $FeWO_4$ composite could offer 98.77% of dye degradation in 90 min (Fig 5c and 6c) due to the synergetic effects between $FeWO_4$ and rGO.

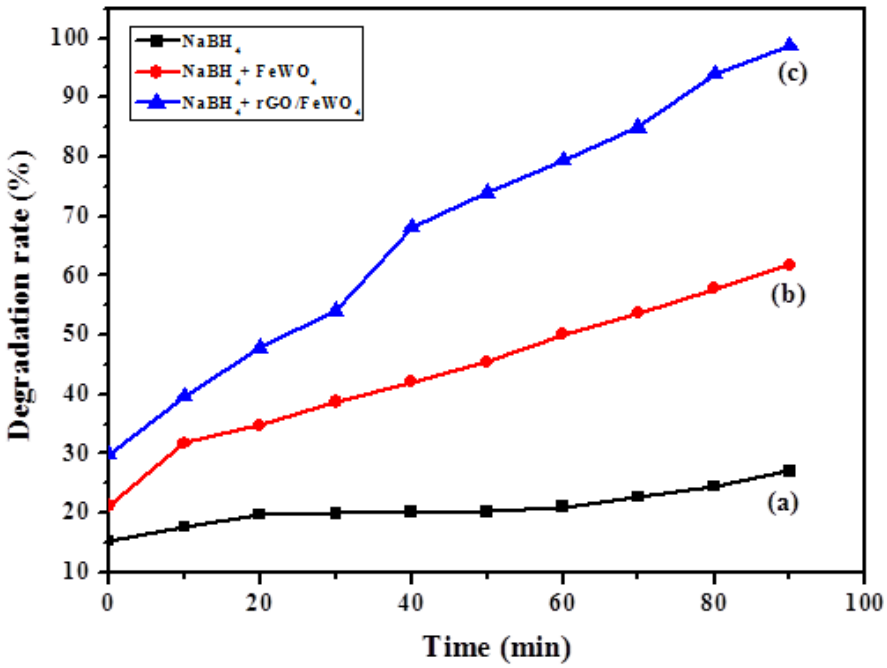

Figure 6 The effect of (a) $NaBH_4$ and $NaBH_4$ mediated (b) $FeWO_4$ (c) rGO/$FeWO_4$ nanosturctures on the degradation of MO dye as a function of time.

The Langmuir-Hinshelwood (L-H) model was applied to study the kinetics of prepared catalytic materials. The L-H equation can be expressed as following when the initial concentration of dye is relatively lower [37].

$$\ln (C_0/C) = Kt$$

where C_0 is the intial concentration of MO, C is the concentration at time t, K is the apparent first-order rate constant and t is the reaction time. **Figure 7** revealed that the plot ln (C_0/C) Vs time is approximately linear. The catalytic degradation of MO dye using prepared nanostructures followed pseudo first-order kinetics and the apparent pseudo first-order rate constants (K) were calculated to be 0.002, 0.008 and 0.038 for $NaBH_4$ and $NaBH_4$ mediated $FeWO_4$ and rGO/ $FeWO_4$ respectively.

The reusability and the cyclic stability of rGO/$FeWO_4$ composite toward MO were recorded and shown in **Figure 8**. The catalyst was separated *via* centrifugation from the dye solution after completion of catalytic reaction, washed several times with water and dried at 90 ^{0}C. The catalytic performance of the catalyst was monitored under identical condition by mixing it with freshly prepared MO dye. The result in Figure8 confirms that the rGO/$FeWO_4$ exhibited a similar catalytic performance without a visible reduction even after 7 cycles, which indicated the stability and long life span of rGO/$FeWO_4$ catalyst.

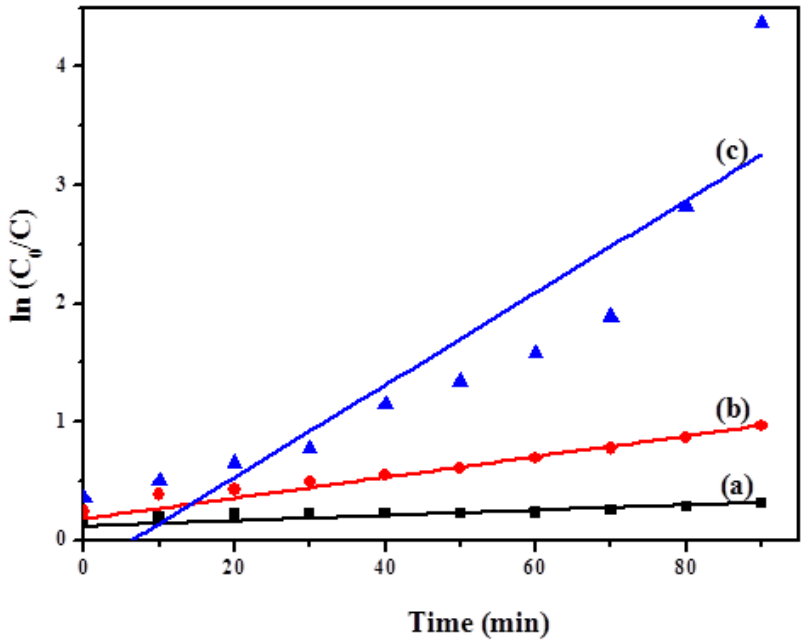

Figure 7 Kinetic linear simulation curves of MO degradation with (a) $NaBH_4$ and $NaBH_4$ mediated (b) $FeWO_4$ (c) rGO/$FeWO_4$ nanostructures.

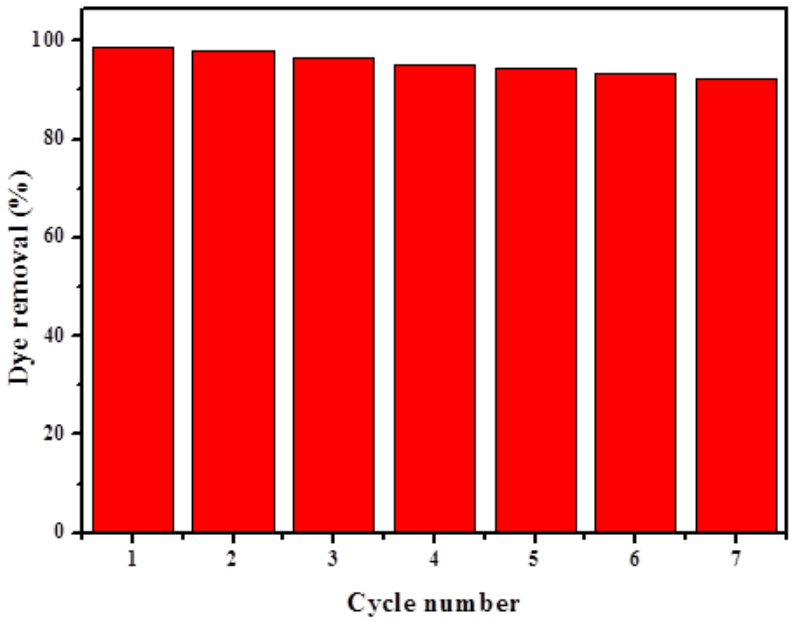

Figure 8 Recyclability of the rGO/$FeWO_4$ nanostructures toward MO dye degradation.

Conclusion

$FeWO_4$ and rGO/$FeWO_4$ nanostructures with flower morphology were developed through the simple solvothermal reaction. The morphological and structural characterizations revealed that the prepared composite exhibited flower like morphological features of $FeWO_4$ with monoclinic primitive structure, uniformly distributed over the rGO sheets. The prepared catalyst materials exhibited catalytic activity towards the degradation of MO dye in the presence of hydride source $NaBH_4$. The high surface area of rGO and exposed active sites of $FeWO_4$ nanosturctures on the surface and the transfer of hydrogen species collectively contributed to the remarkable catalytic activity of rGO/$FeWO_4$. Thus the prepared rGO/$FeWO_4$ catalyst material proved to be good candidate for the degradation of dye pollution in water.

References

[1] S. Yang, Z. Wu, L. P. Huang, B. Zhou, M. Lei, L. Sun, Q. Tian, J. Pan, W. Wu, H. Zhang, Nanoscale Res. Lett., 2014, 9, 442.
[2] W. Lei, D. Portehault, D. Liu, S. Qin, Y. Chen, Nat.Commun., 2013, 4, 1777.
[3] A. Afkhami, R. Moosavi, J. Hazard. Mater., 2010, 174, 398.
[4] Y. H. Shih, C. P. Tso, L. Y. Tung, J. Environ. Eng. Manage. 2010, 20, 137.
[5] Z. C. Kadirova, K. Katsumata, T. Isobe, N. Matsushita, A. Nakajima, K. Okada, Appl. Surf. Sci., 2013, 284, 72.
[6] S. J. Xia, F. X. Liu, Z. M. Ni, J. L. Xue, P. P. Qian, J. Colloid Interface Sci., 2013, 407, 195.
[7] S. Xia, L. Zhang, G. Pan, P. Qian, Z. Ni, Phys. Chem. Chem. Phys., 2015, 17, 5345.
[8] R. Rajesh, S. S. Kumar, R. Venkatesan, New J. Chem., 2014, 38, 1551.
[9] K. Sharma, G. Singh, M. Kumar, V. Bhalla, RSC Adv., 2015, 5, 25781.
[10] T. Shahwana, S. Abu Sirriaha, M. Nairat, E. Boyaci, A. E. Eroglu, T. B. Scott, K. R. Hallam, Chem. Eng. J., 2011, 172, 258.
[11] T. Sinha, M. Ahmaruzzaman, Environ. Sci. Pollut. Res., 2015, 22, 20092.
[12] A. D. Bokare, R. C. Chikate, C. V. Rode, K. M. Paknika, Environ. Sci. Technol., 2007, 41, 7437.
[13] S. M. Gupta, M. Tripathi, Chin. Sci. Bull., 2011, 56, 1639.
[14] V. Sanna, N. Pala, V. Alzari, D. Nuvoli, M. Carcelli, Mater. Lett., 2016, 162, 257.
[15] M. Sharma, T. Jain, S. Singh, O.P. Pandey, Sol. Energ., 2012, 86, 626.
[16] N. E. Fard, R. Fazaeli, R. Ghiasi, Chem. Eng. Technol., 2016, 149.
[17] S. Rajagopal, D. Nataraj, O. Y. Khyzhun, Y. Djaoued, J. Robichaud, D. Mangalaraj, J. Alloys Compd., 2010, 493, 340.
[18] J. Qian, Z. Peng, X. Fu, Chem. Phys. Lett., 2015, 625, 73.
[19] Y.X. Zhou, H.B. Yao, Q. Zhang, J.Y. Gong, S.J. Liu, S. H. Yu, Inorg. Chem., 2009, 48, 1082.
[20] P. Chen, H. Y. He, Res. Chem. Intermed., 2014, 40, 1947.
[21] J. X. Guo, X. Y. Zhou, Y. B. Lu, X. Zhang, S. P. Kuang, W. G. Hou, J. Solid State Chem., 2012, 196, 550.
[22] J. Salamon, Y. Sathishkumar, K. Ramachandran, Y. S. Lee, D. J. Yoo, A.R. Kim, G. Gnanakumar, Biosens. Bioelectron., 2015, 64, 269.
[23] G. Gnanakumar, K. J. Babu, K. S. Nahm, Y. J. Hwang, RSC Adv., 2014, 4, 7944.
[24] C. Liang, T. Zhai, W. Wang, J. Chen, W. Zhao, X. Lu, Y. Tong, J. Mater. Chem. A., 2014, 2, 7214.
[25] G. Gnanakumar, Z. Awan, K. S. Nahm, J. S. Xavier, Biosens. Bioelectron., 2014, 53, 528.
[26] D. Zhang, C. Lu, Y. Ni, Z. Xu, W. Zhang, Cryst. Eng. Comm., 2013, 15, 4755.
[27] A. B. Roney, B. Space, E. W. Castner, R. L. Napoleon, P. B. Moore, J. Phys. Chem. B, 2004, 108, 7389.
[28] B. Yang, Z. Tian, L. Zhang, Y. Guo, S. Yan, J. Water Process Engineering., 2015, 5, 101.
[29] J. Zhang, Y. Wang, S. Li, X. Wang, F. Huang, A. Xie, Y. Shen, Cryst. Eng. Comm., 2011, 13, 5744.
[30] X. Zhou, J. Zhang, H. Wu, H. Yang, J. Zhang, S. Guo, J. Phys. Chem. C., 2011, 115, 11957.
[31] K. Buvaneswari, R. Karthiga, B. Kavitha, M. Rajarajan, A. Suganthi, Appl. Surf. Sci., 2015, 356, 333.
[32] Y. Zhao, X. Song, Q. Song, Z. Yin, Cryst. Eng. Commun., 2012, 14, 6710.
[33] M. Vinothkannan, C. Karthikeyan, G. Gnanakumar, A. R. Kim, D. J. Yoo, Spectrochim. Acta A: Mol. Biomol. Spectrosc., 2015, 136, 256.
[34] B. R. Ganapuram, M. Alle, R. Dadigala, A. Dasari, V. Maragoni, V. Guttena, Int. Nano Lett., 2015, 5, 215.
[35] R. Rajesh, S. S. Kumar, R. Venkatesan, New J. Chem., 2014, 38, 1551.
[36] X. Wang, J. Pauli, R. Niessner, U. R. Genger, D. Knopp, Analyst, 2015, 140, 7305.
[37] R. Shao, L. Sun, L. Tang, Z. Chen, Chem. Eng. J., 2013, 185.

Publication History
Received 04th May 2016
Accepted 12th Jun 2016
Online 30th Oct 2016